

Reactions of *m*-xylene on zeolites with intersecting medium and large pores

Part 2: aluminum population in structures with CON topology

Christopher W. Jones^a, Stacey I. Zones^b, Mark E. Davis^{a,*}

^a Chemical Engineering, California Institute of Technology, Pasadena, CA 91125, USA

^b Chevron Research and Technology Company, Richmond, CA 94802, USA

Received 20 July 1998; accepted 23 November 1998

Abstract

A series of modified SSZ-33 molecular sieves (CON topology) are used as catalysts for the reactions of *m*-xylene. Borosilicate SSZ-33 is transformed into the aluminosilicate form by a low-temperature hydrothermal treatment. Aluminosilicate SSZ-33 samples with different aluminum populations behave similarly in the reactions of *m*-xylene, suggesting that the intracrystalline pore space acts as an ensemble of cages connected by 10- and 12-member rings (MR) rather than intersecting 10-MR and 12-MR channels. Additionally, at low *m*-xylene flow rates, SSZ-33 samples with high Si/Al ratios show an increased amount of transalkylation and the *para/ortho* (*p/o*) and isomerization/disproportionation (*i/d*) selectivities are lower. Reaction over external-surface deactivated SSZ-33 at low flow rates results in unaltered *p/o* ratios. In contrast, reaction over SSZ-33 which contains only aluminum at or near the surface has a greatly decreased *p/o* ratio. The loss in *p/o* and *i/d* selectivity at low flow rates can be attributed to the occurrence of *ortho*-selective bimolecular isomerization at or near the catalyst external surface. © 1999 Elsevier Science B.V. All rights reserved.

Keywords: CON zeolite; Diffusion limitations; External surface; *m*-Xylene

1. Introduction

Zeolites which contain both medium (10-MR) and large (12-MR) pores are currently under investigation as catalysts for a wide variety of reactions (see, e.g., Refs. [1,2]). Molecular sieves which possess the CON (California Institute of Technology number 1) topology such as CIT-1, SSZ-33 (borosilicates as-synthesized) and SSZ-26

(aluminosilicate as-synthesized) contain access to their internal void spaces via 10-MR (5.1 Å × 5.1 Å) and 12-MR (6.4 Å × 7.0 Å) pores [3]. Other zeolites which possess both 10-MR and 12-MR apertures such as NU-87 and SSZ-37 (NES), MCM-22, SSZ-25, ERB-1, PSH-3 and ITQ-1 (MWW) have void spaces which require entrance via the 10-MR alone. In part I of our work, we investigated the catalytic behavior of 10-MR/12-MR zeolites (CIT-1, SSZ-33, SSZ-26, NU-87, MCM-22) by the reactions of *m*-xylene [2]. It is clear that each structure, CON versus

* Corresponding author. Tel.: +1 626 3954251; Fax: +1 626 5688743; E-mail mdavis@cheme.caltech.edu

NES versus MWW, provides for a unique reaction behavior.

Since materials which contain the CON topology have 10-MR and 12-MR pores which are accessible to the intracrystalline void space (see the IZC website for structure: <http://www-iza-sc.csb.yale.edu/IZA-SC/>), it is possible to use these materials to test whether zeolites with intersecting 10-MR and 12-MR pores can be prepared deliberately to simultaneously give the advantageous catalytic behavior of large pores (high diffusion rate) and medium pores (high shape-selectivity and slow deactivation) while not revealing their undesirable characteristics. Previously, we showed that CIT-1 does have a deactivation rate like ZSM-5 [2]: however, the reaction selectivity (*para/ortho* xylene ratio and trimethylbenzene isomer distribution) lies between 10-MR (ZSM-5) and 12-MR (beta) zeolites. Because aluminum is incorporated into SSZ-33 following molecular sieve synthesis, it is possible to control the location of the aluminum in the framework to some extent. Hence, SSZ-33 is a good zeolite candidate to study the effect of aluminum location on reactivity. The objective of the work presented here is to ascertain whether significant differences in aluminum population (and hopefully aluminum siting between 10-MR and 12-MR) alter the reaction behavior of *m*-xylene. Very recently, Sastre et al. [4] reported on the diffusion of *p*-xylene and *o*-xylene in CIT-1 using both molecular dynamics simulations and experimental measurements. Their results suggest that *o*-xylene resides in the 12-MR channels while *p*-xylene accesses both the 12-MR and 10-MR windows under the conditions of their study. If this is the case, and the aluminum population can be manipulated to change the relative number densities in the 12-MR and 10-MR, then the reaction behavior of *m*-xylene should be affected by aluminum siting. However, if the interactions between the 12-MR and 10-MR provide a cage such that the molecular motion at reaction conditions is sufficiently fast so that the entire cage area is accessible during the catalytic transformation, then no variation in reaction behavior with aluminum site distribution is expected. Here, we show that the latter case is the most likely scenario.

2. Experimental

2.1. Catalyst preparation

SSZ-33 (A–D, pE–pH) catalysts were synthesized using endo-N,N,N-trimethyl-8-ammonium tricyclo[5.2.1.0]decane hydroxide as a structure-directing agent (SDA) and Cab-O-Sil M5 fumed silica as the silica source [5]. Samples with varying boron contents were synthesized by adjusting the amount of boron added to the synthesis gels. SSZ-26, an aluminosilicate which is isostructural with SSZ-33, was prepared by direct synthesis using N,N,N,N',N',N'-hexamethyl-8,11-[4.3.3.0]-dodecane diammonium dihydroxide as the SDA [6].

The as-prepared SSZ-33 samples were calcined in air using the following temperature program: heat to 140°C at 2°C min⁻¹ and hold at 140°C for 2 h, heat to 550°C at a heating rate of 1.4°C min⁻¹ and hold at 550°C for 4 h, heat to 610°C at 0.5°C min⁻¹ and hold at 610°C for 2 h, followed by cooling slowly to room temperature. Following calcination, boron was exchanged for aluminum using a low-temperature hydrothermal treatment. In a typical aluminum insertion experiment, 1.2 g of calcined SSZ-33 and 2.87 g of aluminum nitrate nonahydrate were added to 63 ml of H₂O in a plastic bottle. The pH of the solution was near 3.5. The bottle was then sealed with a screw cap and heated in an oven at 95°C statically for three days. Following heating, the pH of the solution was lower (between 1 and 2.5), an event representative of the expulsion of boron and the incorporation of aluminum into the lattice. The solid was then recovered by filtration and washed with 250 ml HCl solution (0.01 M) and 250 ml water to remove any residual boron from the material. The HCl wash ensures that any residual aquated Al³⁺ remains in solution during the filtration. The low pH of the final exchange solution and the HCl wash facilitated exchange of Na⁺ ions for H⁺ ions, negating the need for an ammonium exchange step. The solid was then dried overnight in an oven at ~100°C. After drying, the material was calcined in air using the following temperature program: heat to 175°C at 2.5°C min⁻¹ and hold at 175°C for 2 h, heat to

550°C at 1.25°C min⁻¹ and hold at 550°C for 4 h, followed by cooling slowly to room temperature. For samples where only a portion of the boron sites were exchanged for aluminum, the above procedure was modified by scaling the content of water and aluminum nitrate nonahydrate to obtain the desired Si/Al ratio, assuming that all the aluminum placed into solution was incorporated into the framework. A slight excess of water was used in order to completely wet the zeolite in some cases. Prior to catalysis, all samples were pressed into binder-free pellets, crushed and size-sorted. Particles of a size of -35/+70 were used for catalytic testing. Quartz chips of the same mesh size were used to dilute the catalyst. Quartz was not an active catalyst under the conditions of this study.

2.2. Analytical methods

X-ray powder diffraction (XRD) patterns were collected on a Scintag XDS 2000 diffractometer using Cu K α radiation. Nitrogen adsorption isotherms were obtained at 77 K using an Omnisorp 100 sorption apparatus. ²⁷Al NMR spectra were collected on a Bruker AM 300 spectrometer equipped with a cross-polarization MAS accessory. The ²⁷Al (78.2 MHz) spectra were obtained at a spinning speed of 8 kHz using fully hydrated samples. The spectra were referenced to a 1 M aqueous aluminum nitrate solution. Scanning electron micrographs (SEM) were recorded on a Camscan Series 2-LV scanning electron microscope. X-ray photoelectron spectroscopy (XPS) was performed as described in Ref. [7]. Elemental analyses were performed at Galbraith Laboratories Inc., Knoxville, TN. Catalytic testing was carried out in a downward-flow fixed-bed reactor at 317–318°C and ambient pressure. The catalyst was first activated by heating in a flow of helium (50 ml min⁻¹ STP) to 350°C. Following activation, the reactor temperature was decreased to 317°C over 20 min and the helium was directed through a saturator ($T=10^\circ\text{C}$, $P_{m\text{-xylene}}=3.4$ Torr) containing *m*-xylene (99% Aldrich) absorbed on Chromosorb 102 (Supelco) before flow over the catalyst. The inlet and outlet lines were heated to at least 120°C to prevent reactant/product conden-

Table 1
Physical characteristics of SSZ-33 samples

Sample	Si/B ^a	Si/Al ^b	Si/Al ^c	Si/Al ^d
SSZ-33-A	21.5	20.5	22	22
SSZ-33-B	23	23	23	ND ^e
SSZ-33-C	28.5	24.5	25	ND ^e
SSZ-33-D	32.5	32.5	32.5	ND ^e
pSSZ-33-E	- ^f	29	29.5	29
pSSZ-33-F	- ^f	28	28.5	ND ^e
pSSZ-33-G	- ^f	42.5	43.5	41
pSSZ-33-H	- ^f	87	89	74
SSZ-26	- ^f	13 ^g	13	ND ^e

^aFrom elemental analysis before aluminum insertion.

^bFrom elemental analysis after aluminum insertion.

^cFrom ²⁷Al MAS NMR.

^dFrom XPS.

^eND = not determined.

^fParent sample Si/B = 21.4 or 23.4.

^gAs-synthesized value.

sation in the lines. The contact time (W_{cat}/F_0 ; W_{cat} = weight of catalyst, F_0 = molar flow of *m*-xylene) was varied between 3 and 65 g catalyst h⁻¹ per mol of *m*-xylene. The products were analyzed using an on-line HP 5890 Series II gas chromatograph with a 50 m HP-FFAP column and flame ionization detector. The initial reaction rates and product distributions were obtained by extrapolating the time-dependent data to zero time on-stream.

3. Results and discussion

3.1. Characterization

Two series of catalysts were prepared with different boron populations. For the first series (SSZ-33-A through SSZ-33-D), samples synthesized with different Si/B ratios were completely substituted with Al for B. For the second series, samples with very low Si/B ratios (high boron content) were treated to insert aluminum into only a portion of the vacancies created by boron removal (pSSZ-33-E through pSSZ-33-H; p = partially inserted with aluminum) to give a higher Si/Al ratio. Vacancies not populated with aluminum then remain as silanol nests, as boron is

undetectable by elemental analysis ($<0.1\%$ B). Table 1 lists several characteristics of each sample, including the bulk and surface Si/Al ratios as measured by elemental analysis and XPS, respectively. The bulk composition and surface composition do not show significant variation (possibly a slight surface enrichment of Al for pSSZ-33-H), indicating that the aluminum insertion procedure results in a homogeneous distribution of aluminum in the zeolite even when only a fraction of the boron vacancies are filled. Also included is the Si/Al tetrahedral ratio as ascertained by ^{27}Al MAS NMR, assuming that the populations of tetrahedral and octahedral aluminum measured by this method are reflective of the entire sample. Crystal sizes as measured by SEM were the same for every sample, with cigar-shaped crystals of 1–3 μm in length unless noted. An SEM photo of a typical SSZ-33 sample is given in Fig. 1. Fig. 2 illustrates the XRD pattern of SSZ-33-B, which is representative of the pattern obtained for every sample. All samples had typical nitrogen adsorption capacities near $0.20 \pm 0.015 \text{ ml g}^{-1}$ [8].

3.2. Catalysis

The selectivities of the reactions of *m*-xylene have been used by numerous groups to characterize zeolites [2,9–11]. *m*-Xylene can isomerize into the *para* and *ortho* isomers and can disproportionate

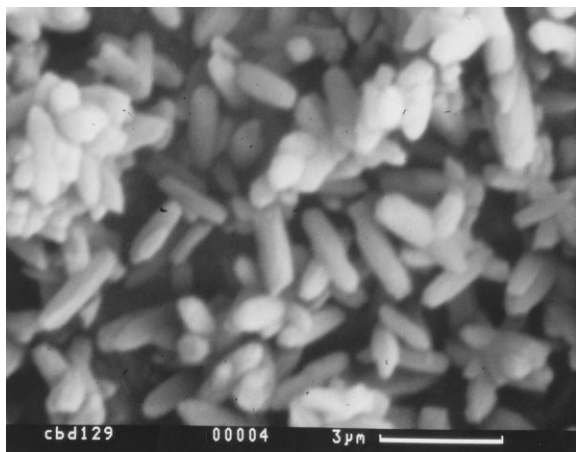


Fig. 1. SEM photograph of SSZ-33-B.

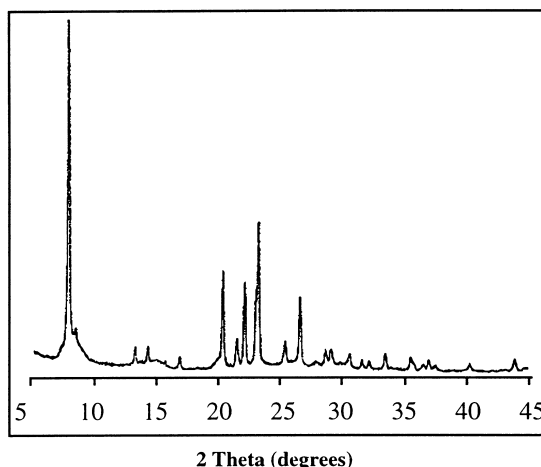
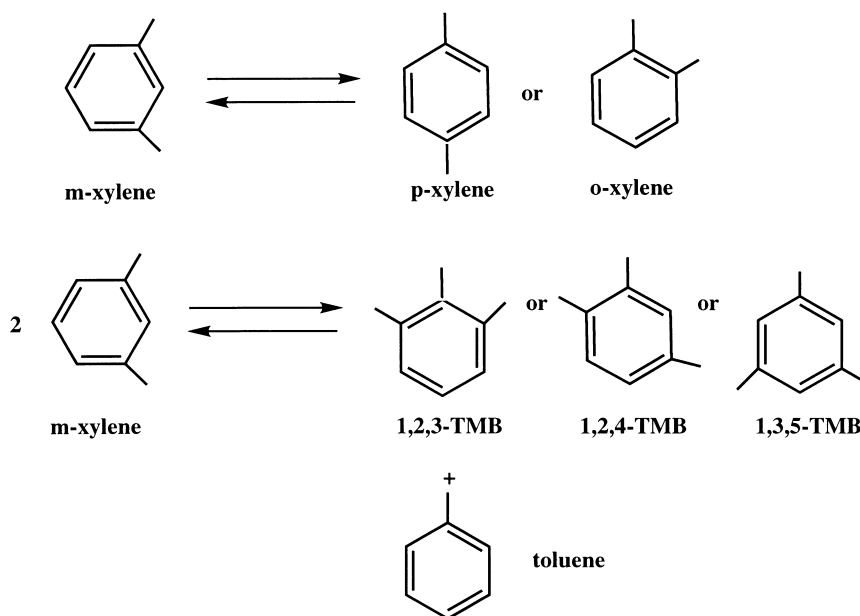


Fig. 2. XRD pattern of SSZ-33-B.

into trimethylbenzenes (TMBs) and toluene, as shown in Scheme 1.

Several key parameters can be ascertained from the results of *m*-xylene reactions over zeolites. The *para*-xylene/*ortho*-xylene product ratio is commonly used for characterizing molecular-sieve pore diameters and architecture [2,9–11]. The *p/o* ratio ranges from >2.5 for 10-MR zeolites like ZSM-5 to <1 for some large and extra-large pore zeolites [9]. The ratio of isomerization to disproportionation (*i/d*) is useful in determining the size of the internal space within a zeolite. Because disproportionation requires a bulky bimolecular transition state, it occurs only to any extent in zeolites with relatively large-sized internal spaces [2,9–11]. In contrast, isomerization normally proceeds via a unimolecular 1,2-methyl-shift mechanism [12], although a bimolecular reaction ($\text{xylene 1} + \text{TMB2} \rightarrow \text{TMB1} + \text{xylene 2}$) is important for zeolites with larger pores [13,14]. This bimolecular reaction allows *p/o* values to fall below 1, as the *p/o* selectivity of the bimolecular isomerization is significantly less than that of the unimolecular reaction (0.28 versus 1.18 for HY) [15]. The distribution of trimethylbenzenes gives information regarding the size of the available pore space within the zeolites. For zeolites with larger pores, the distribution approaches thermodynamic equilibrium. The last parameter which is used to give



information regarding zeolite structure is the rate of deactivation of the zeolite due to coking [2].

Table 2 contains the *p/o* ratio, *i/d* ratio, the distribution of TMBs and the active site–time yield for SSZ-33 and SSZ-26. The active site–time yield (STY) is defined as initial number of molecules of *m*-xylene reacted per active site (assumed equal to

tetrahedral Al) per unit time. It is evident that *p/o* selectivity, *i/d* selectivity and TMB distribution are not affected by the aluminum population, except at higher Si/Al ratios (the reason for the difference at higher Si/Al ratios is discussed below). Specifically striking is the fact that SSZ-33 gives the same product selectivity as SSZ-26. This indi-

Table 2
Product distribution for the reactions of *m*-xylene over SSZ-33 catalysts

Sample	X_0^a	<i>p/o</i> ^b	<i>i/d</i> ^c	Flow rate				STY (h ⁻¹) ^e
				1,2,3 TMB ^d	1,2,4 TMB ^d	1,3,5 TMB ^d	ml STP min ⁻¹	
SSZ-33-A	10.3	1.35	9.5	8.0	71.0	21.0	200	35
SSZ-33-B	12.3	1.37	9.0	8.0	68.5	23.5	200	39
SSZ-33-C	11.5	1.35	10.0	8.0	71.5	20.5	200	25
SSZ-33-D	12.5	1.35	10.0	8.0	72.0	20.0	200	23
pSSZ-33-E	10.5	1.33	12.0	8.0	70.0	22.0	200	38
pSSZ-33-F	9.9	1.32	8.0	8.0	69.0	23.0	155	28
pSSZ-33-G	10.3	1.22	9.0	7.0	72.5	20.5	70	24
pSSZ-33-H	10.1	0.98	6.0	7.0	74.0	19.0	20	9
SSZ-26	13.0	1.32	7.5	8.0	71.5	20.5	200	49

^aInitial conversion.

^bInitial *para/ortho* xylene ratio.

^cInitial isomerization/disproportionation ratio.

^dFraction of TMB isomer (out of 100%).

^eSite–time yield.

cates that the direct incorporation of aluminum into the CON-type structure during synthesis and post-synthetic aluminum insertion into a borosilicate framework both result in a material with the same catalytic selectivity for the reactions of *m*-xylene. It is also apparent that the presence of silanol nests created by boron removal which remain unfilled by aluminum do not significantly affect the selectivity of the reaction (compare SSZ-33-A to pSSZ-33-E and -F). Every sample coked during reaction and there was no obvious difference in the appearance of each sample after reaction. All samples tested deactivated at roughly the same rate. The rates of deactivation for samples SSZ-33-A–pSSZ-33-G and SSZ-26 were determined from the slopes of the plots of *m*-xylene conversion versus time on-stream (slope = %conversion per minute) and all samples deactivated at a rate of $-0.0031 \pm 0.0007\%$ per minute. From these results, it is apparent that from a reaction selectivity perspective, the catalytic behavior of CON zeolites in this study was not altered by the degree of aluminum incorporation. If significant reaction occurred with molecules diffusing through both the 10 and 12-MR channels (if the material behaved as if it had intersecting 10 and 12-MR channels), variations in reactivity with different aluminum populations might be expected. Because aluminum insertion into 12-MRs is significantly easier than insertion into 10-MRs (S.I. Zones, unpublished results), it is expected that the majority of Al is situated at highly accessible sites within the 12-MR pores at low levels of aluminum insertion. Hence, at lower levels of aluminum incorporation, SSZ-33 might be expected to exhibit a selectivity more like 12-MR zeolites. However, the results indicate that the reaction selectivity is essentially the same for samples with a variety of different aluminum contents when the reaction is carried out at sufficiently high flow rates. These results cannot be rationalized by viewing SSZ-33 as a zeolite with intersecting 10 and 12-MR channels. Rather, the material is better described as a zeolite with large cages connected by 10 and 12-MR windows.

The data in Table 2 indicate that the STY is highest for the samples with the most aluminum. This may in part be due to the presence of small

amounts of residual sodium not removed during the aluminum insertion step. The sodium content was determined by elemental analysis for several samples. It was determined that the sodium content was not greatly influenced by the level of aluminum incorporation. Instead, it remained relatively constant (0.1 ± 0.03 wt.%). With a constant amount of sodium, the sodium atoms can be expected to poison a greater percentage of sites in the low aluminum-containing zeolites. It is noteworthy that, with the exception of sample pSSZ-33-H, the variation of STY is not significant for a flow rate in excess of 150 ml min^{-1} ($\pm 10 \text{ h}^{-1}$). pSSZ-33-H contains roughly 0.5 wt.% aluminum (hydrated). It is conceivable that the significantly lower STY for this sample is due to residual sodium (~ 0.1 wt.%). Hence, it is debatable whether a significant trend of STY with aluminum content exists within the error of the measurement.

If the apparent trend is real, the cause could be attributed to other factors in addition to the residual sodium noted above. A similar but more pronounced affect on activity by aluminum content was described for the reaction of *m*-xylene over zeolite beta by Corma and coworkers [16]. The increase in activity with aluminum content over a similar range of Si/Al ratios was concomitant with an increase in *i/d*. This was rationalized by an increased rate of adsorption of the reactant *m*-xylene as the aluminum content increased, causing increased catalytic activity and increased bimolecular reaction (disproportionation). In this work, no significant change in *i/d* is observed, and hence this adsorption effect is probably not important. Another factor to consider is the effect of internal diffusion. Based on a product *p/o* ratio in excess of 1, the reactions of *m*-xylene over CON catalysts are probably affected by internal diffusion. These effects might be expected to be more important over higher-silica materials, as there would be an increased number of adsorption and desorption steps not resulting in reactions at catalytic sites in these materials. Hence, over higher-silica materials, a lower STY could result. It is worth noting that the data showing increased STY with increased aluminum content cannot be rationalized if the structure of SSZ-33 is interpreted as a material with intersecting 10- and 12-MR channels. In this

case, the last aluminum atoms would be expected to incorporate in 10-MR positions, which would probably be less active due to diffusional constraints. In contrast, the results here seem to indicate a slight increase in STY with increasing aluminum content.

As mentioned above, the selectivity of the higher-silica samples pSSZ-33-G and pSSZ-33-H for the runs described in Table 2 are markedly different from the other samples of SSZ-33 and SSZ-26. This is not due to the Si/Al ratio, but instead to the low carrier gas flow rate used for the experiments with these two samples. A lower carrier gas flow rate was initially used to decrease the amount of catalyst needed for these low aluminum-containing catalysts. At low flow rates, the *p/o* and *i/d* ratios are suppressed, as is observed for other zeolites such as USY, SSZ-24 and SSZ-31 [9]. From the data in Table 3, it is evident that at higher flow rates, reaction over pSSZ-33-H yields selectivities which are more in line with the other samples of SSZ-33. Additionally, it appears that flow rate has a large influence on pSSZ-33-H but less influence on the lower-silica SSZ-33-D. This effect can also be observed with other zeolites [9].

The decreased *p/o* selectivity at low flow rates over pSSZ-33-H coincides with a slight increase in activity. The change in activity and selectivity at low flow rates is indicative of external diffusion effects, and implies that the external surface of the zeolite may contribute significantly to overall reaction. Specifically, at low carrier gas flow rates, there may not be a sufficient amount of incoming

m-xylene molecules to effectively facilitate the desorption of products (TMBs) from the catalyst bed. The increased activity may be due to an increased number of transalkylation steps involving a trimethylbenzene reacting with *m*-xylene in a bimolecular isomerization reaction occurring at or near the external surface. Multiple transalkylations are feasible, as 1,2,4-TMB is an order of magnitude more reactive than *m*-xylene over HY [15]. It is evident that there is increased transalkylation at low flows, as the *i/d* ratio is depressed at low flow rates. Guisnet et al. [15] determined that the bimolecular isomerization mechanism (TMB1 + xylene 2 → xylene 1 + TMB2) is selective for the production of the *ortho* isomer of xylene. Thus, increased bimolecular isomerization at or near the surface of the zeolite at low flow rates would explain the lower *p/o* ratio and high active site–time yield obtained under these conditions.

3.3. Catalysis with surface-modified zeolites

To study the influence of external surface reactivity, three samples of SSZ-33 were prepared. SSZ-33-II was prepared such that it contained aluminum only within the zeolite micropores. The as-synthesized borosilicate was treated with trimethylsilylimidazole to cover the external surface. The material was then calcined to remove the SDA. Following calcination, it was subjected to the standard aluminum insertion procedure described above. The surface treatment should cover boron sites on the external surface, prevent-

Table 3
Product distribution for the reactions of *m*-xylene as a function of flow rate

Sample	X_0^a	<i>p/o</i> ^b	<i>i/d</i> ^c	Flow rate	
				(ml STP min ⁻¹)	STY (h ⁻¹) ^d
pSSZ-33-H	10.1	0.98	6.0	20	9.5
	6.4	1.25	13.5	170	6.5
SSZ-33-D	9.0	1.27	5.8	20	19.1
	9.8	1.33	12.0	100	20.1
	12.5	1.35	10.0	200	23.5

^aInitial conversion.

^bInitial *para/ortho* xylene ratio.

^cInitial isomerization/disproportionation ratio.

^dSite–time yield.

ing any subsequent incorporation of aluminum on the outer surface. The material was then calcined again prior to use in reaction experiments. SSZ-33-I2 was prepared such that it contained only internal aluminum using a slightly different approach. This material was first calcined to remove the SDA and then subjected to the standard aluminum insertion procedure. The aluminum-containing zeolite was then treated with trimethylsilylimidazole to cover the external surface aluminum sites. SSZ-33-S was prepared in a manner which populated only the external surface with aluminum atoms, leaving the internal non-silicon framework atoms as boron. As-synthesized B-SSZ-33 was treated using the standard aluminum-insertion procedure. Because the micropores contained SDA during this treatment, it prevented the incorporation of aluminum within the interior of the zeolite. After treatment, the zeolite was calcined to remove the SDA and to generate porosity. The borosilicate form of SSZ-33 is not active for the conversion of *m*-xylene under the conditions used here.

The reaction results, along with some of the physical characteristics of these three samples of SSZ-33, are listed in Table 4. Both samples containing internal aluminum, i.e. SSZ-33-I1 and SSZ-33-I2, have elevated Si/Al ratios as a result of the surface silanation treatments. As expected, SSZ-33-I2, which contained surface aluminum

prior to silanation, has a higher aluminum content than SSZ-33-I1, the sample which had surface boron prior to surface treatment. SSZ-33-S contains only a small amount of aluminum and a large amount of boron, as would be expected if the aluminum insertion treatment affected only the external surface of the zeolite crystals.

In addition to bulk elemental analysis, XPS surface analysis was also performed on these samples. XPS analysis of SSZ-33-S indicated that the surface Si/Al ratio (Si/Al=115) is lower than the bulk value obtained by elemental analysis (Si/Al=190). In addition, the Si/B ratio is nearly that of the as-synthesized sample (Si/B=22 XPS; Si/B=17 as-synthesized), suggesting a selective population of the external surface with aluminum. The X-rays used in XPS analysis penetrate several cages into the crystal, giving information concerning the first few layers of the sample. The fact that a significant amount of boron was detected probably indicates that aluminum insertion into the as-synthesized sample results in population of only the outermost boron sites. It is unlikely that the aluminum is deeper than the first cage. In contrast, XPS analysis of the samples with silanated surfaces indicates that roughly 80% of the boron was removed by the aluminum insertion procedure. This indicates that the majority of the aluminum insertion occurs inside the zeolite when it is accessible. The Si/Al ratio of these samples is near the

Table 4
Characteristics and catalytic results with surface-treated SSZ-33 zeolites

Sample	Si/B ^a	Si/Al ^a	Crystal size ^b (μm)	X ₀ ³	<i>p</i> / <i>o</i> ^d	<i>i</i> / <i>d</i> ^e	Flow rate (ml STP min ⁻¹)
SSZ-33-I1	— ^f	53.3	2–10	8.1	1.74	4.5	20
				8.4	1.71	7.5	100
SSZ-33-I2	— ^g	48	3–6	9.7	1.74	4.0	20
				9.7	1.70	6.2	100
SSZ-33-S	17 ^f	189.5	2–10	9.5	0.95	10.5	20
SSZ-33-I1/S	—	—	—	8.0	1.30	5.0	20

^aAs determined by elemental analysis.

^bCrystal length as determined by SEM.

^cInitial conversion.

^dInitial *para/ortho* xylene ratio.

^eInitial isomerization/disproportionation ratio.

^fB-SSZ-33 parent batch A. Si/B ≈ 17.

^gB-SSZ-33 parent batch B. Si/B ≈ 17.

Parent batches A and B were not otherwise used in this study.

values obtained by bulk elemental analysis. A significant surface silicon enrichment is not detectable by XPS, probably due to the relatively deep penetration depth of the analysis, as noted above. ^{27}Al MAS NMR indicated that the majority of aluminum in SSZ-33-S was tetrahedral (85%).

In the reactions of *m*-xylene, both samples with deactivated surfaces have significantly higher *p/o* ratios than standard SSZ-33 samples such as those described in Tables 1 and 2. It is noteworthy that these samples gave the same product selectivity in the reactions of *m*-xylene despite the fact that different surface deactivation procedures were used. The increased product shape-selectivity for these materials may be attributed to two factors, i.e. deactivation of the zeolite external surface and/or partial pore blockage. There is evidence for a small loss in porosity, as the nitrogen adsorption capacity (77 K) for SSZ-33-I1 is 75% that of SSZ-33-S. It also appears that the *i/d* ratio for the surface-treated samples is slightly depressed compared to standard SSZ-33 samples. While the *i/d* ratio is lowered even further at small flow rates (indicating an increased presence of the reactive TMBs necessary for the bimolecular isomerization mechanism), the *p/o* ratio is virtually unaffected for reaction over SSZ-33-I1 and SSZ-33-I2. This observation supports the hypothesis that at low flow rates, the external surface-mediated bimolecular isomerization is important.

When the surface-aluminum containing sample (SSZ-33-S) is used in the reaction of *m*-xylene at low flow rates, the *p/o* ratio is lowered to 0.95. In addition to this precipitous drop in the *p/o* ratio, it is observed that the *p/o* ratio declines with time on-stream. The data in Fig. 3 illustrate the influence of time on-stream for the *p/o* ratio at low flow rates (20 ml min^{-1}) over various catalysts. The *p/o* ratio for reaction over SSZ-33-D increases slightly with time on-stream. This is expected with zeolites, as deactivation by coking gradually narrows the zeolite pores and makes the catalyst more *para*-selective. Over pSSZ-33-H, a higher-silica sample of SSZ-33 which exhibited a low *p/o* ratio, there is a slight decrease in the *p/o* ratio with time. It appears that a simultaneous decrease in the initial *p/o* ratio and a decreasing *p/o* ratio with time on-stream are indicative of some external

diffusion effects. Similar results have also been obtained with other zeolites at low flow rates [9].

In another experiment, a small portion of SSZ-33-I1 was dispersed in quartz chips and placed over a layer of SSZ-33-S. It was expected that *m*-xylene would react over SSZ-33-I1, generating *para* and *ortho* xylenes and TMBs. The products would then be carried down the bed and into the layer of SSZ-33-S, where TMBs would react on the surface with *m*-xylene to give an overall lower *p/o* ratio than reaction over only SSZ-33-I1. Indeed, this is what results (Table 4). While reaction over only SSZ-33-I1 gives a high *para* selectivity, the presence of SSZ-33-S and its reactive surface reduces the *p/o* ratio to 1.3. Additionally, it is observed that the *p/o* ratio drops with time on-stream to values well below 1, as illustrated in Fig. 3. A lower *p/o* ratio and *i/d* ratio, higher STY, and a declining *p/o* ratio with time on-stream are all observed at low flow rates and are indicative of external diffusional limitations.

The effect of external diffusion on *p/o* ratio at low flow rates is not as pronounced for all catalysts. The lower-silica SSZ-33-D has essentially the same *p/o* ratio at low and high flow rates, while the higher-silica pSSZ-33-H is markedly affected by the flow rate (Table 3). In general, high-silica zeolites or relatively inactive zeolites (activity per g of catalyst) are affected to a greater degree by flow rate. This could be due to the fact that to obtain a given conversion, a larger mass of catalyst is generally required for a high-silica zeolite (low density of acid sites) as compared to a low-silica zeolite (high density of acid sites). Therefore, in order to maintain a relatively constant conversion at constant temperature, a deeper bed is usually needed for high-silica zeolites. This deeper bed allows for an increased probability for secondary adsorption events preventing primary products from escaping the catalyst. As a result, there appears to be increased surface mediated bimolecular isomerization for higher-silica samples. However, low flow rates do not change the reaction selectivity for all high-silica zeolites. Flow rate is also found to have little or no affect on the *p/o* selectivity of the high-silica zeolites ZSM-12 and SSZ-35 [9]. Because TMBs are required for the bimolecular isomerization mechanism, smaller-

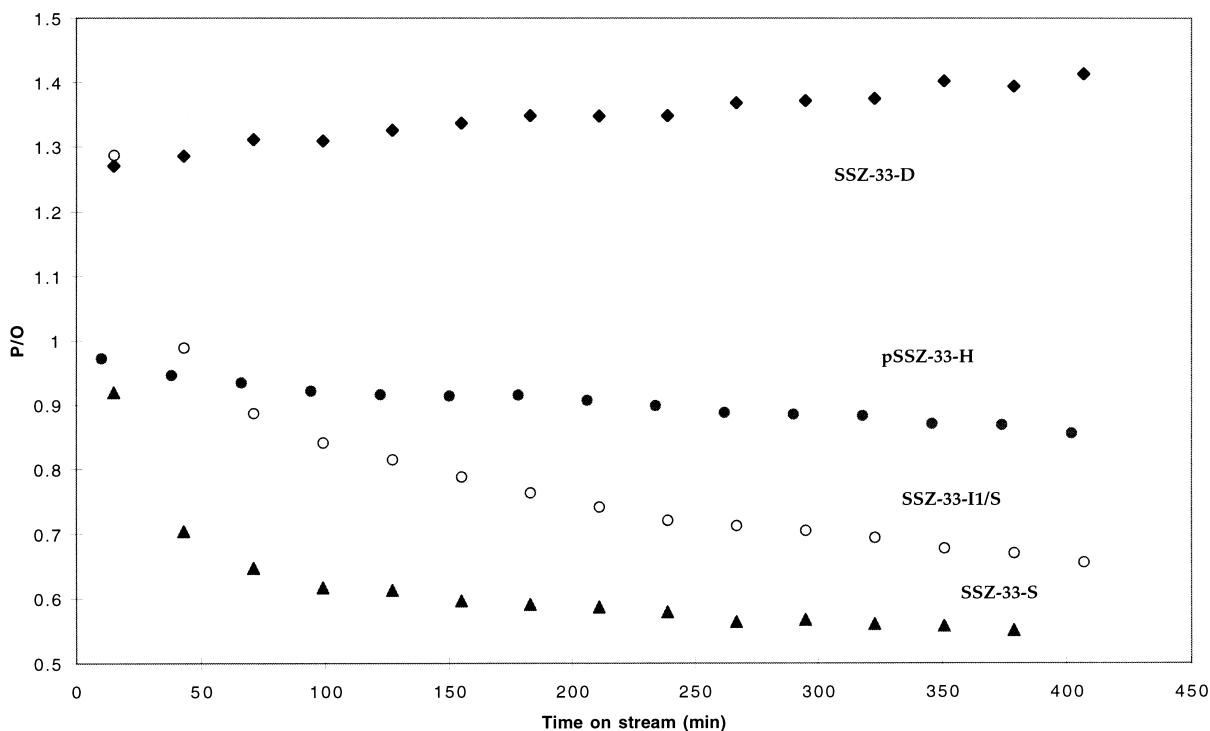


Fig. 3. *m*-Xylene conversion versus time on stream. The carrier gas flow rate was 20 ml min⁻¹.

pore zeolites which produce fewer TMBs (ZSM-12, SSZ-35) are less likely to be affected by the flow rate.

There are no reports of *p/o* ratios below 1 where the unimolecular isomerization mechanism is ascribed to be the origin of the catalytic behavior. This is because *m*-xylene is transformed to *para* and *ortho* xylene at similar rates by the unimolecular 1,2-methyl shift mechanism in the absence of diffusional limitations [12]. Over amorphous aluminosilicates, only the unimolecular isomerization mechanism operates and the *p/o* selectivity is in excess of 1 (1.4 in Ref. [17]). In addition, the *p/o* selectivity of the unimolecular mechanism over HY was found to be 1.18 by Guisnet et al. [15]. Thus, under conditions without significant internal or external diffusional limitations, the unimolecular isomerization mechanism results in *p/o* ratios near or slightly in excess of 1. Hence, *p/o* ratios below 1 may be attributed to isomerization products resulting from the bimolecular transalkylation mechanism.

4. Summary

SSZ-33 catalysts with boron completely replaced by aluminum and SSZ-33 catalysts which have only a portion of the boron vacancies replaced by aluminum give similar catalytic selectivities in the reactions of *m*-xylene. This indicates that the CON structure behaves more like an ensemble of large cages connected by 10- and 12-MR windows rather than a material with intersecting 10- and 12-MRs.

At low flow rates, higher-silica SSZ-33 catalysts are strongly affected by external diffusional limitations. Under these conditions, the *p/o* and *i/d* selectivities are lowered. SSZ-33 samples with a deactivated external surface do not give a smaller *p/o* ratio. In contrast, samples with aluminum only at or near the external surface give a significantly lower *p/o* ratio at low flow rates. The loss in *p/o* and *i/d* selectivities at low flow rates can be attributed to external diffusional limitations which probably do not allow for the rapid desorption of primary products from the zeolite surface. Under

these conditions, the primary products can undergo further reaction at or near the surface, specifically the *ortho*-selective bimolecular isomerization reaction.

Acknowledgements

The authors thank Dr. Sheilah Yeh for performing the XPS analysis and Lun Teh Yuen for the synthesis of the surface-modified SSZ-33. This work was supported by the Chevron Research and Technology Company. C.W.J. thanks Akzo Nobel for financial support.

References

- [1] A. Corma, M.E. Davis, V. Fornes, V. Gonzalezalvaro, R. Lobo, A.V. Orchilles, *J. Catal.* 167 (1997) 438–446.
- [2] B. Adair, C.Y. Chen, K.T. Wan, M.E. Davis, *Microporous Mater.* 7 (1996) 261–270.
- [3] W.M. Meier, D.H. Olson, Ch. Baerlocher, *Atlas of Zeolite Structure Types*, Structure Commission IZA, 4th ed., Elsevier, London, 1996.
- [4] G. Sastre, N. Raj, R.A. Catlow, R. Roque-Malherbe, A. Corma, *J. Phys. Chem. B* 102 (1998) 3198–3209.
- [5] S.I. Zones, US Patent 4 963 337, 1990.
- [6] S.I. Zones, M.M. Olmstead, D.S. Santilli, *J. Am. Chem. Soc.* 114 (1992) 4195–4201.
- [7] M. Yoshikawa, S.I. Zones, M.E. Davis, *Microporous Mater.* 11 (1997) 137–148.
- [8] Y. Nakagawa, G.S. Lee, T.V. Harris, L.T. Yuen, S.I. Zones, *Microporous Mesoporous Mater.* 22 (1998) 69–85.
- [9] C.W. Jones, S.I. Zones, M.E. Davis, *Appl. Catal. A*, in press.
- [10] J. Weitkamp, S. Ernst, *Catal. Today* 19 (1994) 107–150.
- [11] J.A. Martens, J. Perez-Pariente, E. Sastre, A. Corma, P.A. Jacobs, *Appl. Catal. A* 45 (1988) 85–101.
- [12] A. Cortes, A. Corma, *J. Catal.* 51 (1978) 338–344.
- [13] A. Corma, E. Sastre, *J. Catal.* 129 (1991) 177–185.
- [14] A. Corma, E. Sastre, *J. Chem. Soc., Chem. Commun.* (1991) 594–596.
- [15] S. Morin, N.S. Gnep, M. Guisnet, *J. Catal.* 159 (1996) 296–304.
- [16] J. Perez-Pariente, E. Sastre, V. Fornes, J.A. Martens, P.A. Jacobs, A. Corma, *Appl. Catal.* 69 (1991) 125–137.
- [17] S. Morin, P. Ayrault, S. El Mouahid, N.S. Gnep, M. Guisnet, *Appl. Catal. A* 159 (1997) 317–331.